Viscosity in hot scalar field theory

Enke Wang* and Ulrich Heinz
Institut für Theoretische Physik, Universität Regensburg, D-93040 Regensburg, Germany

Xiaofei Zhang
Institute of Particle Physics, Hua-Zhong Normal University, Wuhan 430070, China
(Received 17 August 1995; revised manuscript received 12 January 1996)

The spectral representation for general two-point Green functions in thermo field dynamics is used to compute the spectral density of the ϕ^2-ϕ^2 correlation function in hot ϕ^4 theory. We give a compact derivation of the one-loop contribution to the shear viscosity and show that it is dominated by low-momentum plasmons. The weak-coupling behavior of the viscosity is strongly influenced by the momentum dependence of the plasmon width. [S0556-2821(96)02710-5]

PACS number(s): 11.10.Wx, 51.10.+y, 52.25.Fi, 52.60.+h

In the context of heavy-ion collisions at high energies, the transport properties of strongly interacting hot matter, in particular, of the quark-gluon plasma (QGP), have become an issue of intense theoretical interest. The calculation of the QGP transport coefficients from linear response functions through the Kubo formalism [1,2] has so far been hampered by infrared problems associated with the nonlinear self-interactions among massless fields in hot QCD. A systematic and economic field theoretical approach, including infrared resummation techniques [3], to the calculation of linear response functions, is clearly asked for.

As an example, consider the Kubo formula for the shear viscosity [1,4,5]:

$$\eta = -\frac{1}{5}\int d^3x' \int_{-\infty}^{0} dt \int_{-\infty}^{t} dt' \langle \pi^{\mu\nu}(0), \pi_{\mu\nu}(\mathbf{x}',t') \rangle^{\rm ret}$$

$$= \frac{\pi}{5} \lim_{\omega,\mathbf{p}\to 0} [\partial \rho_{\pi\pi}(\omega,\mathbf{p})/\partial\omega]. \qquad (1)$$

$\pi_{\mu\nu}$ is the traceless viscous-pressure tensor, which in the comoving frame has only spatial components π_{ij}. For a scalar field, $\pi_{ij} = (\delta_{ik}\delta_{jl} - 1/3\ \delta_{ij}\delta_{kl})\partial_k\phi\partial_l\phi$. $\rho_{\pi\pi}$ is the spectral momentum space density for the retarded thermal Green function of the composite field π, as defined below. The efficient computation of this quantity will be the subject of this paper.

The analytical structure of the retarded Green function $\langle \pi^{\mu\nu}(0), \pi_{\mu\nu}(\mathbf{x}',t') \rangle^{\rm ret}$ is similar to that of $\langle \phi^2(0), \phi^2(\mathbf{x}',t') \rangle^{\rm ret}$ [5]. The spectral density for the latter object was recently calculated at one-loop order in the imaginary time formalism (ITF) by Jeon [5]. We redo the calculation in the real-time formalism using the language of thermo field dynamics (TFD) [6,7]. Using the analytic properties of the two-point functions in ITF and TFD, we give a compact derivation of the one-loop contribution to the spectral density of the composite field two-point function $\rho_{\pi\pi}$ in terms of the spectral density of the elementary field two-point function, $\rho_{\phi\phi}$. The latter was recently calculated at two-loop order including infrared resummation [5,8,9]. Our approach goes beyond the results reported in [5] in that we include the full momentum dependence of the two-loop scalar self-energy.

Let us first summarize a few analytical relations for the full propagators in the different finite temperature formalisms for later use. For two arbitrary operators $\hat{A}$, $\hat{B}$, the *retarded thermal Green function* is defined by

$$D^{\rm ret}_{AB}(\mathbf{r}_1-\mathbf{r}_2, t_1-t_2) = -i\theta(t_1-t_2)\mathrm{Tr}(e^{\beta(\Omega-\hat{H})} \times [\hat{A}(\mathbf{r}_1,t_1), \hat{B}(\mathbf{r}_2,t_2)]_{\pm}), \qquad (2)$$

where $\hat{H}$ is the Hamiltonian, Ω is the thermodynamic potential, and the plus (minus) sign applies for fermionic (bosonic) operators $\hat{A}$, $\hat{B}$. In momentum space it has the following spectral representation in terms of the spectral density $\rho_{AB}(\omega,\mathbf{p})$:

$$D^{\rm ret}_{AB}(p_0,\mathbf{p}) = \lim_{\eta\to 0^+} \int_{-\infty}^{+\infty} d\omega \frac{\rho_{AB}(\omega,\mathbf{p})}{p_0 - \omega + i\eta} = [D^{\rm adv}_{AB}(p_0,\mathbf{p})]^*. \qquad (3)$$

The second equality defines the *advanced thermal Green function*. The same spectral density also generates the *imaginary time (ITF) Green function* which is obtained from Eq. (2) by setting $it = \tau$. In momentum space,

$$G_{AB}(\omega_n,\mathbf{p}) = \int_{-\infty}^{+\infty} d\omega \frac{\rho_{AB}(\omega,\mathbf{p})}{i\omega_n - \omega}, \qquad (4)$$

where ω_n are the discrete Matsubara frequencies. The retarded and ITF Green functions are related by analytical continuation, $i\omega_n \to p_0 + i\eta$.

The real time propagators in TFD have a more complicated 2×2 matrix structure. As discussed in Ref. [7], there is a continuous infinity of representations of thermo field dynamics which are all equivalent in global thermal equilibrium. However, for fermionic fields a consistent dynamical theory connecting different thermal equilibrium states and, a fortiori, a consistent kinetic theory can only be developed [7] on the basis of the ''linear'' ($\alpha = 1$) representation rather

*On leave of absence from Institute of Particle Physics, Hua-Zhong Normal University, Wuhan, China.

than the original ''symmetric'' ($\alpha=1/2$) representation [6] of TFD. In this representation, the TFD propagator in momentum space takes for bosonic operators the form [7]

$$\Delta^{ab}_{AB}(p_0,\mathbf{p})=\mathscr{B}^{-1}\begin{pmatrix} D^{\rm ret}_{AB}(p_0,\mathbf{p}) & \\ & D^{\rm adv}_{AB}(p_0,\mathbf{p})\end{pmatrix}\mathscr{B}\tau_3, \quad (5)$$

where

$$\mathscr{B}=\begin{pmatrix} 1+n(p_0) & -n(p_0)\\ -1 & 1\end{pmatrix}, \quad (6)$$

$\tau_3=\mathrm{diag}(1,-1)$, and $n(p_0)=[\exp(\beta p_0)-1]^{-1}$ is the Bose distribution. Explicitly, Eq. (5) reads

$$\Delta^{ab}_{AB}(p_0,\mathbf{p})=\begin{pmatrix} D^{\rm ret}_{AB}(p_0,\mathbf{p})-2\pi i n(p_0)\rho_{AB}(p_0,\mathbf{p}) & -2\pi i n(p_0)\rho_{AB}(p_0,\mathbf{p})\\ -2\pi i[1+n(p_0)]\rho_{AB}(p_0,\mathbf{p}) & -D^{\rm adv}_{AB}(p_0,\mathbf{p})-2\pi i n(p_0)\rho_{AB}(p_0,\mathbf{p})\end{pmatrix}. \quad (7)$$

Similar expressions for fermionic correlation functions are given in Sec. 3.3.2 of Ref. [7].

Equation (7) provides a particularly straightforward way of extracting the spectral density

$$\rho_{AB}(p_0,\mathbf{p})=\frac{i}{2\pi}(e^{\beta p_0}-1)\Delta^{12}_{AB}(p_0,\mathbf{p}). \quad (8)$$

The 12-component of the two-point Green function can be calculated directly using the TFD Feynman rules. Using the Schwinger-Dyson equation [10] for the full TFD propagator (we now drop the indices A,B for clarity),

$$(\Delta^{-1})^{ab}=(p^2-m^2)\tau_3^{ab}+\Sigma^{ab}(p_0,\mathbf{p}), \quad (9)$$

it is straightforward to relate the components of the 2×2 TFD self-energy matrix Σ^{ab} to the self-energy Σ of the analytically continued ITF propagator. For example, the spectral density is related to the ITF self-energy by

$$\rho(p_0,\mathbf{p})=-\frac{1}{2\pi i}[D^{\rm ret}(p_0,\mathbf{p})-D^{\rm adv}(p_0,\mathbf{p})]=\frac{1}{\pi}\frac{\mathrm{Im}\Sigma(p_0,\mathbf{p})}{[p^2-m^2+\mathrm{Re}\Sigma(p_0,\mathbf{p})]^2+[\mathrm{Im}\Sigma(p_0,\mathbf{p})]^2}. \quad (10)$$

We will now use these results to give a three line derivation of the spectral function for the composite field ϕ^2 within hot $\lambda\phi^4$ theory. We concentrate on the same quantity as studied in Ref. [5], namely,

$$\eta_{\phi^2\phi^2}\equiv\lim_{\mathbf{p},p_0\to0}[\rho_{\phi^2\phi^2}(p_0,\mathbf{p})/p_0], \quad (11)$$

whose relation to the shear viscosity (1) was mentioned above. Equation (8) tells us that we must calculate $\Delta^{12}_{\phi^2\phi^2}(p_0,\mathbf{p})$. The lowest order contribution is shown diagrammatically in Fig. 1. This is a skeleton diagram, i.e., the full single-particle propagator must be used for the internal lines [1,5]. For the one-loop diagram in Fig. 1 only its 12-component is needed. We find

$$i\Delta^{12}_{\phi^2\phi^2}(p_0,\mathbf{p})=2\int\frac{d^4k}{(2\pi)^2}n(k_0)\rho_{\phi\phi}(k_0,\mathbf{k})n(p_0-k_0)\times\rho_{\phi\phi}(p_0-k_0,\mathbf{p}-\mathbf{k}). \quad (12)$$

Combining this with Eqs. (8) and (11), we obtain

$$\eta^{1\ \rm loop}_{\phi^2\phi^2}=2\beta\int\frac{d^4k}{(2\pi)^3}n(k_0)[1+n(k_0)][\rho_{\phi\phi}(k_0,|\mathbf{k}|)]^2, \quad (13)$$

where we used $n(-k_0)=-[1+n(k_0)]$ as well as

$$\rho_{\phi\phi}(\omega,\mathbf{p})=\mathrm{sgn}(\omega)\rho_{\phi\phi}(|\omega|,|\mathbf{p}|), \quad (14)$$

which follows from spatial isotropy and CPT invariance of the thermal equilibrium state [5]. The factor β results from $\lim_{p_0\to0}(e^{\beta p_0}-1)/p_0$. Equation (13) agrees, up to a factor 2π because of our different normalization (10) of the spectral density, with the ITF calculation of Ref. [5].

To further evaluate Eq. (13), we need the spectral density $\rho_{\phi\phi}(k_0,\mathbf{k})$ for the full single-particle propagator. Since the calculation of $\eta^{1\ \rm loop}_{\phi^2\phi^2}$ requires taking the zero-momentum limit of the loop diagram, both internal lines in Fig. 1 can become soft. To avoid infrared divergences in massless $\lambda\phi^4$ theory, we should thus use resummed effective propagators [3,8]. The so-called resummation of ''hard thermal loops'' [3] in this case generates a thermal mass for the scalar field which acts as an infrared cutoff. Using such a resummation scheme, we performed in [9] a two-loop calculation of $\rho_{\phi\phi}$. We found that for weak coupling ($\lambda/24\ll1$), the spectral function is sharply peaked around the plasmon frequency:

$$\omega_p(\mathbf{k})=\sqrt{\mathbf{k}^2+m_{\rm th}^2-3m_{\rm th}^3/\pi T}\equiv\sqrt{\mathbf{k}^2+m_p^2}, \quad (15)$$

where $m_{\rm th}=T\sqrt{\lambda/24}$ is the ''thermal mass'' and m_p is the plasmon mass [8]. $\rho_{\phi\phi}$ can then be well approximated by a relativistic Breit-Wigner function

$$\rho_{\phi\phi}(k_0,\mathbf{k})\approx\frac{1}{\pi}\frac{2k_0\gamma(\mathbf{k})}{[k_0^2-\omega_p^2(\mathbf{k})]^2+4k_0^2\gamma^2(\mathbf{k})}, \quad (16)$$

with the on-shell damping rate for the scalar plasmon

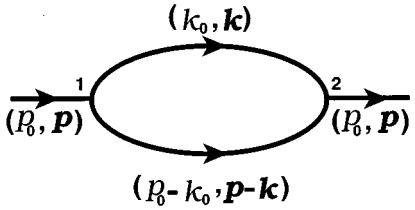

FIG. 1. One-loop skeleton diagram for $\Delta^{12}_{\phi^2\phi^2}(p_0,\mathbf{p})$. The heavy lines denote full single-particle propagators.

$$\gamma(\mathbf{k})=\frac{\mathrm{Im}\Sigma[\omega_p(\mathbf{k}),\mathbf{k}]}{2\omega_p(\mathbf{k})}. \tag{17}$$

Substituting Eq. (16) into Eq. (13) and integrating over k_0, we obtain [1,5,12]

$$\eta^{1\,\mathrm{loop}}_{\phi^2\phi^2}\approx\frac{\beta}{2\pi}\int\frac{d^3k}{(2\pi)^3}\,\frac{n[\omega_p(\mathbf{k})]\{1+n[\omega_p(\mathbf{k})]\}}{\omega_p^2(\mathbf{k})\,\gamma(\mathbf{k})}. \tag{18}$$

The leading (two-loop) contribution to (17) reads [9,11]

$$\gamma(\mathbf{k})=\frac{\lambda^2T^2}{256\ \pi^3\omega_p(\mathbf{k})}\ A(x;a), \tag{19}$$

where

$$A(x;a)=\frac{1}{x}\int_0^x dz\Bigg[L_2(\xi)+L_2\left(\frac{\xi-\zeta}{\xi(1-\zeta)}\right)-L_2\left(\frac{\xi-\zeta}{1-\zeta}\right)-L_2\left(\frac{(\xi-\zeta)(1-\xi\zeta)}{\xi(1-\zeta)^2}\right)\Bigg], \tag{20}$$

with

$$x=\beta|\mathbf{k}|,\quad a=\beta m_p,\quad \xi=e^{-\sqrt{x^2+a^2}},\quad \zeta=e^{-\sqrt{z^2+a^2}}, \tag{21}$$

and the Spence function (dilogarithm)

$$L_2(z)\equiv-\int_0^z dt\,\frac{\ln(1-t)}{t}. \tag{22}$$

A plot of the function $A(x;a)$ can be found in Figs. 36 and 37 of Ref. [11]. For large momenta, $x\to\infty$, it approaches the constant value [11]

$$\lim_{x\to\infty}A(x;a)=\begin{cases}\pi^2/6 & \text{for}\quad a\to0,\\ aK_1(a) & \text{for}\quad a\gg1,\end{cases} \tag{23}$$

while at zero momentum it takes the value [11] $A(0;a)=L_2(e^{-a})$ which again goes to $\pi^2/6$ in the weak-coupling limit $a\to0$ $(\lambda\to0)$.

We now evaluate the momentum integral in (18). It can be studied analytically in the weak-coupling limit $\lambda\ll1$. Let us begin by neglecting as in [2,5] the momentum dependence of the plasmon width, i.e., by replacing $\gamma(\mathbf{k})$ in (18) by

$$\gamma(0)=\frac{\lambda^2T^2}{1536\pi m_p}[1+O(\sqrt{\lambda}\ln\lambda)]. \tag{24}$$

Partial integration then leads to

$$\eta^{1\,\mathrm{loop}}_{\phi^2\phi^2|\,\gamma(0)}=\frac{384\,a^3}{\pi^2T\lambda^2}\int_0^\infty\frac{dx}{(x^2+a^2)^{3/2}}\,\frac{1}{e^{\sqrt{x^2+a^2}}-1},$$

with $a=m_p/T$. For $a\ll1$, this integral can be evaluated following Ref. [13], and we obtain [14]

$$\eta^{1\,\mathrm{loop}}_{\phi^2\phi^2|\,\gamma(0)}\approx\frac{96}{\pi T}\,\frac{1}{\lambda^2}\left(1-\sqrt{\frac{\lambda}{6\pi^2}}+O(\lambda)\right). \tag{25}$$

With the explicit momentum dependence (19) of the plasmon decay width, this approximation can be avoided. Integrating Eq. (18) by parts, we find

$$\eta^{1\,\mathrm{loop}}_{\phi^2\phi^2|\,\gamma(\mathbf{k})}=\frac{64}{\lambda^2T}\int_0^\infty\frac{dx}{e^{\sqrt{x^2+a^2}}-1}\,\frac{A(x;a)-xA'(x;a)}{A^2(x;a)}, \tag{26}$$

where the prime denotes d/dx. Unfortunately, for weak coupling, the function $A(x;a)$ exhibits a very strong momentum dependence in the region $a<x<1$; for $a=0$, the limit $x\to0$ is nonanalytic. To get an idea of the structure of the integral, let us first neglect the momentum dependence of A (i.e., of the self-energy Σ). Then

$$\eta^{1\,\mathrm{loop}}_{\phi^2\phi^2}\approx\frac{64}{\lambda^2T}\,\frac{6}{\pi^2}\int_0^\infty\frac{dx}{e^{\sqrt{x^2+a^2}}-1}. \tag{27}$$

In the limit $a\to0$, this integral diverges logarithmically in the infrared. The singularity can be isolated by writing

$$\begin{aligned}\int_0^\infty\frac{dx}{e^{\sqrt{x^2+a^2}}-1}&=\int_a^\infty\frac{\varepsilon}{\sqrt{\varepsilon^2-a^2}}\,\frac{d\varepsilon}{e^\varepsilon-1}\\&=\int_a^\infty\frac{d\varepsilon}{e^\varepsilon-1}+\int_a^\infty\frac{\varepsilon-\sqrt{\varepsilon^2-a^2}}{\sqrt{\varepsilon^2-a^2}}\,\frac{d\varepsilon}{e^\varepsilon-1}\\&=-\ln(1-e^{-a})\\&\quad+\int_a^\delta\frac{\varepsilon-\sqrt{\varepsilon^2-a^2}}{\sqrt{\varepsilon^2-a^2}}\,\frac{d\varepsilon}{\varepsilon}+O\left(\frac{a^2}{\delta^2}\right)\\&=\ln\left(\frac{1}{a}\right)+\ln2+O(a)+O\left(\frac{a^2}{\delta^2}\right).\end{aligned} \tag{28}$$

In the fourth line we cut off the second integral at the upper end at a point δ with $a\ll\delta\ll1$. This allows the approximation of the Bose distribution as $1/\varepsilon$. The remaining integral from δ to ∞ is finite and of order a^2/δ^2. We thus find, with this approximation [14],

$$\begin{aligned}\eta^{1\,\mathrm{loop}}_{\phi^2\phi^2}&\approx\frac{384}{\pi^2T}\,\frac{1}{\lambda^2}\left[\ln\left(\frac{T}{m_p}\right)+\ln2\ +O\left(\frac{m_p}{T}\right)\right]\\&=\frac{192}{\pi^2T}\,\frac{1}{\lambda^2}\left[\ln\left(\frac{1}{\lambda}\right)+\ln(96)+O(\sqrt{\lambda})\right].\end{aligned} \tag{29}$$

The additional logarithmic divergence in the weak-coupling limit of (29) compared to (25) is generic; its coefficient and the next-to-leading constant term depend, how-

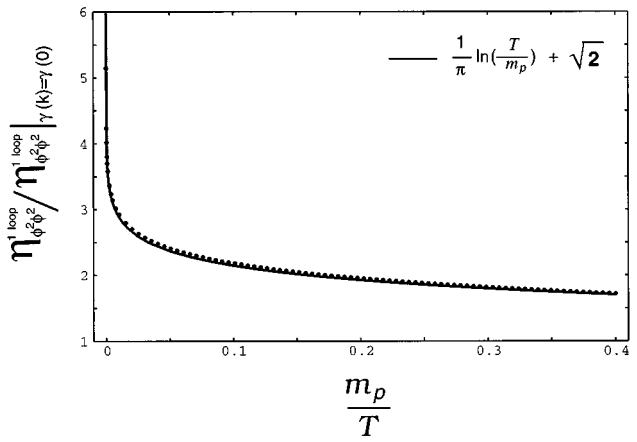

FIG. 2. The dots represent numerical results for the ratio between $\eta^{1\ \mathrm{loop}}_{\phi^2\phi^2}|_{\gamma(\mathbf{k})}$ and $\eta^{1\ \mathrm{loop}}_{\phi^2\phi^2}|_{\gamma(0)}$ as a function of m_p/T. The solid line indicates a fit of the form $(1/\pi)\ln(T/m_p)+\sqrt{2}$.

ever, on the (so far neglected) momentum dependence of $A(x;a)$. Because of the nonanalytic behavior of $A(x;0)$ near $x=0$, we did not succeed in extracting an analytical expression similar to (29) for the full integral (26). The numerical result shown by the dots in Fig. 2 can, however, be excellently fit by

$$\frac{\eta^{1\ \mathrm{loop}}_{\phi^2\phi^2}|_{\gamma(\mathbf{k})}}{\eta^{1\ \mathrm{loop}}_{\phi^2\phi^2}|_{\gamma(0)}} = 0.3282\ \ln\left(\frac{T}{m_p}\right) + 1.41682 \approx \frac{1}{\pi}\ln\left(\frac{T}{m_p}\right) + \sqrt{2}, \tag{30}$$

which suggests the analytical behavior

$$\eta^{1\ \mathrm{loop}}_{\phi^2\phi^2}|_{\gamma(\mathbf{k})} = \frac{96}{\pi^2 T}\frac{1}{\lambda^2}\left[\ln\left(\frac{T}{m_p}\right) + \pi\sqrt{2} + O\left(\frac{m_p}{T}\right)\right] = \frac{48}{\pi^2 T}\frac{1}{\lambda^2}\left[\ln\left(\frac{1}{\lambda}\right) + \ln(24) + 2\pi\sqrt{2} + O(\sqrt{\lambda})\right]. \tag{31}$$

As intuitively expected, the viscosity decreases as the coupling strength increases: In relaxation time approximation, all transport coefficients are proportional to the relaxation time, which again is inversely proportional to the scattering rate which grows with the coupling strength. On the other hand, the rate at which our $\eta_{\phi^2\phi^2}$ decreases with the coupling strength λ, is different from the behavior of the physical shear viscosity η. As discussed in the introduction, the latter involves four additional spatial derivatives acting on the scalar field. This translates [1] into an additional factor k^4 in the integrand of Eq. (18), which removes the infrared divergence of this integral in the limit $a\to 0$ and thereby also the leading logarithmic term in our final result (31). This observation provides a partial explanation for the qualitatively different behavior of the viscosity as a function of m_p/T which was recently found by Jeon in a more complete study of $g\phi^3+\lambda\phi^4$ theory [11]: his numerical results indicate an increase of $\lambda^2\eta$ with increasing λ.

Still, as first pointed out by Jeon in [5] and then quantitatively analyzed in [11], the fact that the shear viscosity η is proportional to $1/\lambda^2$ raises a serious problem: simple power counting arguments [5] show that then an infinite series of planar ladder diagrams can also contribute to the leading order result for the viscosity. Its summation is nontrivial and has been recently performed by Jeon [11] using the imaginary time formalism. This work was a genuine *tour de force*, and the prospect of generalizing it to non-Abelian gauge theories, such as QCD, seems frightening. We expect that efficient use of the analyticity properties of the full propagators as demonstrated here in the framework of TFD will help to streamline the calculation and facilitate its generalization to QCD.

We are grateful to P. Henning, Liu Lianshou, Li Jiarong, and R. D. Pisarski for helpful discussions. This work was supported by DFG, BMBF, NSFC, and GSI.

[1] A. Hosoya, M.-A. Sakagami, and M. Takao, Ann. Phys. (N.Y.) **154**, 229 (1984).
[2] S.V. Ilyin, A.D. Panferov, and Yu. Sinyukov, Phys. Lett. B **227**, 455 (1989); S.V. Ilyin, O.A. Mogilevsky, S. Smolyanski, and G.M. Zinovjev, *ibid.* **296**, 385 (1992).
[3] R.D. Pisarski, Phys. Rev. Lett. **63**, 1129 (1989); E. Braaten and R.D. Pisarski, Nucl. Phys. **B337**, 569 (1990).
[4] D.N. Zubarev, *Nonequilibrium Statistical Thermodynamics* (Plenum, New York, 1974).
[5] S. Jeon, Phys. Rev. D **47**, 4586 (1993).
[6] H. Umezawa, H. Matsumoto, and M. Tachiki, *Thermo Field Dynamics and Condensed States* (North-Holland, Amsterdam, 1982).
[7] P.A. Henning, Phys. Rep. **253**, 235 (1995).
[8] R.R. Parwani, Phys. Rev. D **45**, 4695 (1992).
[9] E. Wang and U. Heinz, Phys. Rev. D **53**, 899 (1996).
[10] H. Matsumoto, I. Ojima, and H. Umezawa, Ann. Phys. (N.Y.) **152**, 348 (1984).
[11] S. Jeon, Phys. Rev. D **52**, 3591 (1995).
[12] Yu.S. Gangnus, A.V. Prozorkevich, and S.A. Smolyanski, Theor. Math. Phys. **35**, 321 (1978).
[13] L. Dolan and R. Jackiw, Phys. Rev. D **9**, 3320 (1974).
[14] Our result should be compared with Eq. (5.12) in Ref. [5]. If in that expression the mass is replaced by m_p, it exhibits a logarithmic dependence $\sim\lambda^{-2}\ln(\tilde{a}\lambda)$ on the coupling constant. Our calculation [see Eqs. (25) and (29)] shows that this result (with $\tilde{a}=2$) is obtained if the momentum dependence of the plasmon's *self-energy* (and not of the plasmon *width* as erroneously stated in Ref. [5]) is neglected.